J|A|C|S
ARTICLES
Published on Web 05/18/2006

Conformational Changes during Apoplastocyanin Folding Observed by Photocleavable Modification and Transient Grating

Shun Hirota,*[,†,‡] Yukari Fujimoto,[§,||] Jungkwon Choi,[⊥] Naoki Baden,[⊥] Noriko Katagiri,[§] Masako Akiyama,[§] Rinske Hulsker,[¶] Marcellus Ubbink,[¶] Toshihide Okajima,[#] Teruhiro Takabe,[£] Noriaki Funasaki,[†] Yoshihito Watanabe,[§] and Masahide Terazima*[,⊥]

Contribution from the Department of Physical Chemistry, 21st Century COE Program, Kyoto Pharmaceutical University, 5 Nakauchi-cho, Misasagi, Yamashina-ku, Kyoto 607-8414, Japan, PRESTO, Japan Science and Technology Agency, Kawaguchi, Saitama 332-0012, Japan, Department of Chemistry, Graduate School of Science, Nagoya University, Chikusa-ku, Nagoya 464-8602, Japan, Department of Chemistry, Graduate School of Science, Kyoto University, Sakyo-ku, Kyoto 606-8502, Japan, Leiden Institute of Chemistry, Gorlaeus Laboratories, Leiden University, P.O. Box 9502, 2300 RA Leiden, The Netherlands, Institute of Scientific and Industrial Research, Osaka University, Ibaraki, Osaka 567-0047, Japan, and Research Institute, Meijo University, Tempaku-ku, Nagoya 468-8502, Japan

Received December 28, 2005; E-mail: hirota@mb.kyoto-phu.ac.jp; mterazima@kuchem.kyoto-u.ac.jp

Abstract: A new method to investigate the initial protein folding dynamics is developed based on a pulsed laser light triggering method and a unique transient grating method. The side chain of the cysteine residue of apoplastocyanin (apoPC) was site-specifically modified with a 4,5-dimethoxy-2-nitrobenzyl derivative, where the CD and 2D NMR spectra showed that the modified apoPC was unfolded. The substituent was cleaved with a rate of about 400 ns by photoirradiation, which was monitored by the disappearance of the absorption band at 355 nm and the increase in the transient grating signal. After a sufficient time from the photocleavage reaction, the CD and NMR spectra showed that the native β-sheet structure was recovered. Protein folding dynamics was monitored in the time domain with the transient grating method from a viewpoint of the molecular volume change and the diffusion coefficient, both of which reflect the global structural change, including the protein−water interaction. The observed volume decrease of apoPC with a time scale of 270 μs is ascribed to the initial hydrophobic collapse. The increase in the diffusion coefficient (23 ms) is considered to indicate a change from an intermolecular to an intramolecular hydrogen bonding network. The initial folding process of apoPC is discussed based on these observations.

Introduction

Proteins form their unique three-dimensional structures to function in organisms. Although both experimental and theoretical studies on the protein folding character have been performed extensively in the past decades,[1−4] the protein folding dynamics has not been well elucidated. For the kinetic study of the protein folding, we should accomplish two important points: initiation and detection of the refolding process.[5−17] For example, stopped flow, rapid mixing, laser-induced temperature jump, and light-induced electron injection methods have been used for the

† Kyoto Pharmaceutical University.
‡ PRESTO, JST.
§ Nagoya University.
⊥ Kyoto University.
¶ Leiden University.
# Osaka University
£ Meijo University.
|| Present address: Department of Chemistry, Graduate School of Science, Osaka University, Toyonaka, Osaka 560-0043, Japan.

(1) Baldwin, R. L. *Nat. Struct. Biol.* **1999**, *6*, 814−817.
(2) Baldwin, R. L.; Rose, G. D. *Trends Biochem. Sci.* **1999**, *24*, 77−83.
(3) Dill, K. A.; Chan, H. S. *Nat. Struct. Biol.* **1997**, *4*, 10−19.
(4) Onuchic, J. N.; Wolynes, P. G.; Luthey-Schulten, Z.; Socci, N. D. *Proc. Natl. Acad. Sci. U.S.A.* **1995**, *92*, 3626−3630.
(5) Telford, J. R.; Wittung-Stafshede, P.; Gray, H. B.; Winkler, J. R. *Acc. Chem. Res.* **1998**, *31*, 755−763.
(6) Chen, E.; Wittung-Stafshede, P.; Kliger, D. S. *J. Am. Chem. Soc.* **1999**, *121*, 3811−3817.
(7) Jones, C. M.; Henry, E. R.; Hu, Y.; Chan, C.-K.; Luck, S. D.; Bhuyan, A.; Roder, H.; Hofrichter, J.; Eaton, W. A. *Proc. Natl. Acad. Sci. U.S.A.* **1993**, *90*, 11860−11864.
(8) Akiyama, S.; Takahashi, S.; Ishimori, K.; Morishima, I. *Nat. Struct. Biol.* **2000**, *7*, 514−520.
(9) Uzawa, T.; Akiyama, S.; Kimura, T.; Takahashi, S.; Ishimori, K.; Morishima, I.; Fujisawa, T. *Proc. Natl. Acad. Sci. U.S.A.* **2004**, *101*, 1171−1176.
(10) Yeh, S.-R.; Han, S.; Rousseau, D. L. *Acc. Chem. Res.* **1998**, *31*, 727−736.
(11) Yeh, S.-R.; Ropson, I. J.; Rousseau, D. L. *Biochemistry* **2001**, *40*, 4205−4210.
(12) Shastry, M. C. R.; Roder, H. *Nat. Struct. Biol.* **1998**, *5*, 385−392.
(13) Capaldi, A. P.; Shastry, M. C. R.; Kleanthous, C.; Roder, H.; Radford, S. E. *Nat. Struct. Biol.* **2001**, *8*, 68−72.
(14) Abbruzzetti, S.; Viappiani, C.; Small, J. R.; Libertini, L. J.; Small, E. W. *J. Am. Chem. Soc.* **2001**, *123*, 6649−6653.
(15) Hofrichter, J. *Methods Mol. Biol.* **2001**, *168*, 159−191.
(16) Dyer, R. B.; Gai, F.; Woodruff, W. H.; Gilmanshin, R.; Callender, R. H. *Acc. Chem. Res.* **1998**, *31*, 709−716.
(17) Vu, D. M.; Myers, J. K.; Oas, T. G.; Dyer, R. B. *Biochemistry* **2004**, *43*, 3582−3589.

initiation, and flash photolysis of an organic cross-linker has been shown to be a useful method by Chan and co-workers.[18,19] For the detection, the extent of protein denaturation has been frequently monitored by visible or IR absorbance, emission, circular dichroism (CD), resonance Raman measurements, and so on. Changes in emission and absorbance intensities, which are associated with the optical transition, provide us information on a rather local structural change around the chromophores, whereas formation of the secondary structure (e.g., α-helices or β-sheets) can be monitored by the CD and IR signal intensities. However, to understand the nature or the mechanism of protein folding, it is essential to monitor the global protein structural change and/or the protein−solvent interaction, for example, hydrophobic or hydrogen bonding interaction, in the time domain. In this paper, we report a novel approach to study the protein folding kinetics. For triggering the folding reaction, a denaturant is photodissociated from a protein by a pulsed laser.[20] For monitoring the folding process, the time developments of the molecular volume change as well as the diffusion coefficient, which are difficult to detect by conventional spectroscopy, are monitored by the transient grating (TG) method. Combining these methods, we succeeded in investigating the dynamics of protein conformation as well as the protein−water intermolecular interaction during the initial protein folding process of a β-sheet structure.

Two mechanisms for protein folding, the hydrophobic collapse mechanism[21] and the hierarchic mechanism,[2,22] have been proposed. In the hydrophobic collapse mechanism, the folding begins with the protein collapse, whereas helices are formed before the final collapse in the hierarchic mechanism. Simulation studies on helical proteins have shown that the actual folding step for a protein can depend on the experimental conditions.[23,24] Although it is well-known that the solvent effect plays an important role not only in chemical reactions but also in protein structures and functions, little is known on the interaction between the protein and water molecules during protein folding.

Plastocyanin (PC) functions as an electron transfer protein in photosynthetic organisms.[25−27] PC exhibits an overall structure of a β-barrel composed of two β-sheets with eight strands and a single turn of an α-helix.[28−31] It contains a copper atom, which is coordinated with a sulfur atom of the unique cysteine. Refolding of Cu-depleted PC (apoPC) has been shown to include two slow steps corresponding to isomerization from *trans* to *cis* of the two prolines,[32,33] but its faster folding reaction has not been investigated. We, therefore, chemically modified apoPC with a 4,5-dimethoxy-2-nitrobenzyl (DMNB) group, which exhibits an absorption band at 355 nm, and studied the early events in the β-sheets' refolding process of apoPC.

Experimental Section

Protein Modification. *Silene pratensis* PC was purified as described.[34,35] PC (∼40 μM) in 20 mM Na phosphate buffer (∼40 mL), pH 7.4, containing 1 M NaCl and 0.1 mM EDTA was placed under nitrogen atmosphere, followed by an addition of sodium dithionite (0.0348 g) dissolved in a small amount of the same buffer. Dithionite was removed from the solution by dialysis, and the dialyzed solution was placed under nitrogen atmosphere again. To remove the copper atom from the protein, the protein solution was stirred with 50 mM KCN at 4 °C for 12 h under nitrogen atmosphere. KCN was removed by dialysis with 20 mM Na phosphate buffer, pH 7.4, containing 2 mM 2-mercaptoethanol, and the protein solution was finally dialyzed with 20 mM Na phosphate buffer, pH 7.4. To obtain ^{15}N-labeled PC, *E. coli* cells were cultured in M9 minimal medium containing $(^{15}NH_4)_2SO_4$, and the copper atom was removed from ^{15}N-labeled PC by the same procedure. For additional ^{13}C labeling, 1 g/L of ^{13}C-labeled glucose was present in the medium.

Chemical modification of apoPC was carried out by mixing apoPC in 20 mM Na phosphate buffer (45 μM, 1 mL), pH 7.4, and 4,5-dimethoxy-2-nitrobenzyl bromide in dimethylformamide (4.5 mM, 100 μL) under nitrogen atmosphere. The mixed solution was stirred at 50 °C for 15 min under nitrogen atmosphere in the dark. The DMNB-modified apoPC was stirred with 50 mM dithiothreitol in the dark and then dialyzed with 10 mM Na phosphate buffer, pH 7.4.

The DMNB-modified and unlabeled apoPCs were separated using a DEAE sephacel column at 4 °C in the dark. Unlabeled apoPC eluted from the column with 10 mM Na phosphate buffer, pH 7.4, containing 100 mM NaCl, while modified apoPC started to elute from the column only with higher NaCl concentration (10 mM Na phosphate buffer, pH 7.4, containing 300 mM NaCl). Elution of the modified protein was confirmed by the absorption spectrum, which exhibited an absorption band at 355 nm due to the DMNB derivative. The obtained DMNB-modified apoPC solution was dialyzed with 10 mM Na phosphate buffer, pH 7.4. A photoreactive model peptide, DMNB-modified *N*-acetyl-Asp-Gly-Cys, was obtained by performing the same reaction as that for the modified apoPC.

Protein Digestion, MALDI-TOF MS Analysis, and Amino Acid Sequence Determination. The DMNB-modified apoPC (0.6 mg, 30 μM) in 100 mM ammonium bicarbonate buffer, pH 8 (2 mL), was digested with lysyl endopeptidase (Lys-C from *Achromobacter lyticus*, Wako Ltd., Osaka, Japan) (5 μg) in 100 mM Tris-HCl buffer, pH 8.0 (10 μL), at 37 °C for 17 h in the dark. ApoPC was also digested in the same manner. The peptide mixtures resulting from Lys-C digestion of the DMNB-modified and unlabeled apoPCs were fractioned by HPLC: column, shin-pack PREP-ODS(H) (Shimadzu, Kyoto, Japan) 250 × 10 mm; flow rate, 0.8 mL/min; detection, absorption at 215, 280, and 355 nm; mobile phase, linear 60 min gradient from 0 to 60% solvent B in solvent A (solvent A, 0.1% TFA−H_2O; solvent B, 0.1% TFA−CH_3CN). Major peaks were collected manually. The mass spectra of the collected peptides from the Lys-C digestion were measured with a MALDI-TOF MS spectrometer (PerSeptive Biosystems, Voyager) in a linear mode with a N_2 laser, using α-cyano-4-hydroxycinnamic acid as a matrix. The DMNB-modified peptide fraction was further analyzed by the post-source decay mode to obtain the sequence

(18) Chen, R. P.-Y.; Huang, J. J.-T.; Chen, H.-L.; Jan, H.; Velusamy, M.; Lee, C.-T.; Fann, W.; Larsen, R. W.; Chan, S. I. *Proc. Natl. Acad. Sci. U.S.A.* **2004**, *101*, 7305−7310.
(19) Kuo, N. N.-W.; Huang, J. J.-T.; Miksovska, J.; Chen, R. P.-Y.; Larsen, R. W.; Chan, S. I. *J. Am. Chem. Soc.* **2005**, *127*, 16945−16954.
(20) Okuno, T.; Hirota, S.; Yamauchi, O. *Biochemistry* **2000**, *39*, 7538−7545.
(21) Dill, K. A. *Biochemistry* **1985**, *24*, 1501−1509.
(22) Baldwin, R. L.; Rose, G. D. *Trends Biochem. Sci.* **1999**, *24*, 26−33.
(23) Boczko, E. M.; Brooks, C. L., III. *Science* **1995**, *269*, 393−396.
(24) Zhou, Y.; Karplus, M. *Nature* **1999**, *401*, 400−403.
(25) Sykes, A. G. *Struct. Bonding (Berlin)* **1991**, *75*, 175−224.
(26) Redinbo, M. R.; Yeates, T. O.; Merchant, S. *J. Bioenerg. Biomembr.* **1994**, *26*, 49−66.
(27) Gross, E. L. *Photosynth. Res.* **1993**, *37*, 103−116.
(28) Colman, P. M.; Freeman, H. C.; Guss, J. M.; Murata, M.; Norris, V. A.; Ramshaw, J. A. M.; Venkatappa, M. P. *Nature* **1978**, *272*, 319−324.
(29) Guss, J. M.; Freeman, H. C. *J. Mol. Biol.* **1983**, *169*, 521−563.
(30) Guss, J. M.; Harrowell, P. R.; Murata, M.; Norris, V. A.; Freeman, H. C. *J. Mol. Biol.* **1986**, *192*, 361−387.
(31) Freeman, H. C. In *Coordination Chemistry−21*; Laurent, J. L., Ed.; Pergamon Press: Oxford, U.K., 1981; Vol. 21, pp 29−51.
(32) Koide, S.; Dyson, H. J.; Wright, P. E. *Biochemistry* **1993**, *32*, 12299−12310.
(33) Mizuguchi, M.; Kroon, G. J.; Wright, P. E.; Dyson, H. J. *J. Mol. Biol.* **2003**, *328*, 1161−1171.
(34) Hirota, S.; Hayamizu, K.; Endo, M.; Hibino, T.; Takabe, T.; Kohzuma, T.; Yamauchi, O. *J. Am. Chem. Soc.* **1998**, *120*, 8177−8183.
(35) Hirota, S.; Hayamizu, K.; Okuno, T.; Kishi, M.; Iwasaki, H.; Kondo, T.; Hibino, T.; Takabe, T.; Kohzuma, T.; Yamauchi, O. *Biochemistry* **2000**, *39*, 6357−6364.

information. The amino acid sequence of the isolated DMNB-modified peptide was determined with a protein sequencer (Applied Biosystems, 491HT).

Absorption, Circular Dichroism, and NMR Measurements. Absorption and CD spectra of the protein (17 μM) in 10 mM Na phosphate buffer, pH 7.4, containing 1 mM dithiothreitol (DTT) were measured immediately after purification at room temperature on a Shimadzu UV 3101PC spectrophotometer and a Jasco J-720 spectropolarimeter in quartz cells with path lengths of 10 and 2 mm, respectively. DTT was added to the protein solution to trap the generated nitrosobenzyl compound and to prevent it from reacting with the protein. Low-intensity 355 nm pulses were obtained from the third harmonic of an Nd:YAG laser (Continuum, Minilite II; pulse energy, 3 mJ/cm^2; pulse width, 5 ns).

For NMR measurements, the DMNB-modified apoPC was dissolved in 10 mM sodium phosphate buffer, pH 7.4. Irradiation with 355 nm laser pulses was preformed in the presence of 2 mM dithiothreitol, and the obtained protein was dialyzed and concentrated with Amicon in the same buffer. NMR spectra were recorded at 600 MHz on a Bruker DMX spectrometer at 302 K. Resonances in the heteronuclear single-quantum coherence (HSQC) spectrum of apoPC were assigned using 3D triple-resonance experiments, HNCACB and HN(CA)CO.

Transient Grating Measurements. The third harmonic of an Nd:YAG laser (Spectra-Physics, Quantum-ray Model GCR-170-10) with a 10 ns pulse was used as an excitation beam to create the transient grating (TG).[36,37] The excitation beam was divided into two beams with a beam splitter, and they were crossed inside the sample solution. A He−Ne (633 nm) or a diode (840 nm) laser beam was used as a probe beam. The diffracted probe beam was isolated from the excitation laser beam with a glass filter (Toshiba, R-60) and a pinhole. The TG signal was detected by a photomultiplier tube (Hamamatsu, R-928) and fed into a digital oscilloscope (Tetronix, TDS-520). The signal was averaged by a microcomputer to improve the signal-to-noise ratio (S/N). The energy entering the sample was adjusted below 5 μJ/pulse. The sample solution was renewed after every 200 shots of the excitation laser pulses.

The repetition rate of the excitation laser was less than 1 Hz to prevent possible bleaching of the reactant and to dissipate the photoproduct away from the excitation region. The size of the excitation beam at the sample position was ca. 1 mm ϕ. The irradiated volume was small (typically ca. 4×10^{-3} cm^3) compared with the entire volume of the sample solution. All measurements were carried out at room temperature.

Principle and Theoretical Analysis. A photoinduced reaction takes place by the sinusoidally modulated light intensity that is produced by the interference of two excitation light waves. The spatial modulation in the concentration of the reactant and the product leads to the sinusoidal modulation in the refractive index change (δn) and absorbance change (δk), and this modulation can be monitored by the diffraction efficiency of the probe beam (TG signal).[36,38−45] When the absorbance change is negligible at the probe wavelength, the TG signal intensity is proportional to the square of the refractive index change.

$$I_{TG}(t) = \alpha \delta n(t)^2 \qquad (1)$$

where α is a proportional constant that represents the sensitivity of the system. The refractive index change is mainly caused by the released thermal energy (thermal grating) and the created (or depleted) chemical species by the photoreaction (species grating). The signal intensity becomes weaker as the spatial modulations of the refractive index become uniform, which is accomplished by the translational diffusion. Hence, the decay rate constant of the thermal grating signal should be given by $D_{th}q^2$ (D_{th}, thermal diffusivity of the solution; q, grating wavenumber ($q = 2\pi/\Lambda$, Λ is the fringe spacing of the grating)). The species grating signal decays with a rate constant of Dq^2, where D is the diffusion coefficient of the chemical species. When D of the reactant (D_r) and the product (D_p) are time-independent, the time development of the TG signal can be expressed by a biexponential function.[38−41]

$$I_{TG}(t) = \alpha\{\delta n_r \exp(-D_r q^2 t) + \delta n_p \exp(-D_p q^2 t)\}^2 \qquad (2)$$

where δn_r (<0) and δn_p (>0) are the refractive index changes due to the presence of the reactant and the product, respectively. The signs of δn_r and δn_p are negative and positive, respectively, because the phase of the spatial concentration modulation of the reactant is 180° shifted from that of the product. It is important to note here that, once the spatial distribution of the chemical species becomes uniform by the diffusion, the signal should disappear. Therefore, the time range we can observe with the TG signal depends on $D_r q^2$ or $D_p q^2$ (the smaller one). In other words, the observation time range is determined for a given D by the magnitude of q^2.

Results

Identification of Modified Amino Acid. The fragments obtained by Lys-C digestion of the DMNB-modified and unlabeled apoPCs were purified by HPLC. By comparing the HPLC profiles of the peptide fractions obtained from the DMNB-modified and unlabeled apoPCs, a new fragment with an absorption peak at 355 nm appeared for the DMNB-modified apoPC, while a fragment with a shorter retention time than this new fragment disappeared (Figure 1). The absorption at 355 nm of the new fragment corresponds to that of the DMNB group. The MALDI-TOF MS ion peak of the new fragment was detected at m/z 1604.4, whereas that of the fragment of the unlabeled apoPC missing for the DMNB-modified apoPC was observed at m/z 1409.2. The difference in the mass between these two fragments was m/z 195.2, which corresponded very well with the molecular weight of the DMNB group. These results show that the modified amino acid was included in this peptide fragment. No other peptide fragment was perturbed significantly in the HPLC profile, which showed that the protein is modified only at a single position of this fragment.

By performing peptide sequence analysis of this peptide, it was shown that this peptide corresponds to the amino acids from 82 to 95, and only the third residue from the N-terminal of this peptide, cysteine (Cys84), is modified. The molecular ion peak of m/z 1604.4 and the MS/MS spectrum of this peptide were in agreement with this assignment. These results indicate that the unique cysteine of apoPC is attached to a DMNB group in the modified protein. In addition, Ellman's test showed that there was no free cysteine sulfur atom for the modified protein, which supports that the cysteine residue is modified.

Photocleavage of DMNB Group from Modified Protein and Induced Protein Structural Change. The absorption band at 355 nm of the modified protein is attributed to the DMNB derivative (Figure 2A). This band disappeared by irradiation with 355 nm laser pulses on the DMNB-modified protein, which shows that the DMNB group is removed from the protein by irradiation of the pulses. Instead, the absorption at 280 nm

(36) Nada, T.; Terazima, M. *Biophys. J.* **2003**, *85*, 1876−1881.
(37) Nishida, S.; Nada, T.; Terazima, M. *Biophys. J.* **2004**, *87*, 2663−2675.
(38) Okamoto, K.; Terazima, M.; Hirota, N. *J. Chem. Phys.* **1995**, *103*, 10445−10452.
(39) Terazima, M.; Hirota, N. *J. Chem. Phys.* **1993**, *98*, 6257−6262.
(40) Takeshita, K.; Imamoto, Y.; Kataoka, M.; Tokunaga, F.; Terazima, M. *Biochemistry* **2002**, *41*, 3037−3048.
(41) Choi, J.; Terazima, M. *J. Phys. Chem. B* **2002**, *106*, 6587−6593.
(42) Fayer, M. D. *Annu. Rev. Phys. Chem.* **1982**, *33*, 63−87.
(43) Miller, R. J. D. *Annu. Rev. Phys. Chem.* **1991**, *42*, 581−614.
(44) Eichler, H. J.; Gunter, P.; Pohl, D. W. *Laser Induced Dynamic Gratings*; Spirnger-Verlag: Berlin, 1986.
(45) Choi, J.; Terazima, M. *J. Phys. Chem. B* **2003**, *107*, 9552−9557.

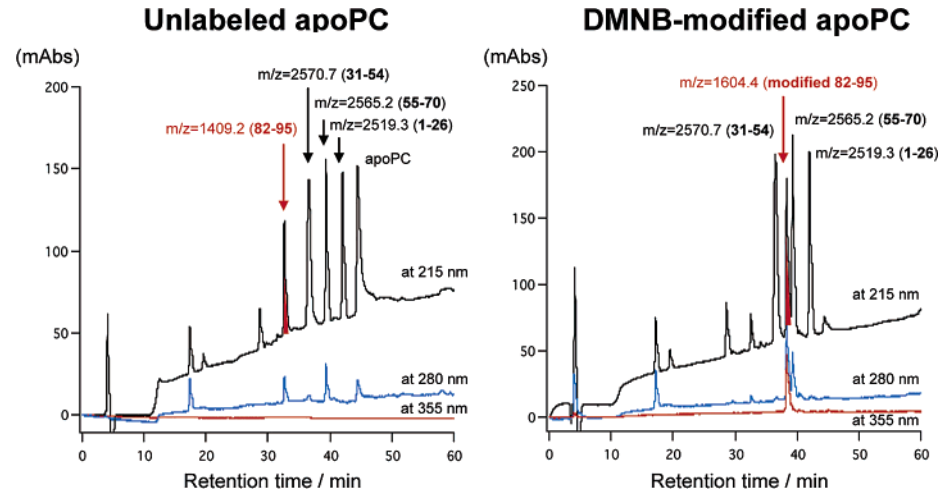

Figure 1. HPLC profiles of the unlabeled and DMNB-modified apoPCs cleaved by lysl endopeptidase together with the mass of the fragments obtained by MALDI-TOF MS measurements. Absorptions at 215 (black line), 280 (blue line), and 355 (red line) nm were monitored.

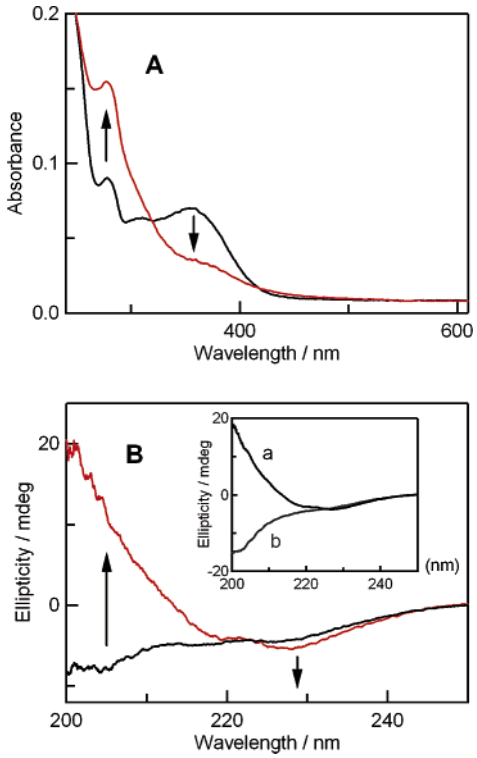

Figure 2. Absorption and CD spectra for the DMNB-modified apoPC before (black line) and after (red line) 10 min of irradiation with weak 355 nm laser pulses (10 Hz, 3 mJ/cm^2): (A) absorption and (B) CD spectra. DMNB-modified apoPC (8 μM) was dissolved in 10 mM sodium phosphate buffer, pH 7.4, with 1 mM DTT. (Inset) CD spectra for (a) native (pH 7.4) and (b) acid-denatured (pH 2.0) apoPC.

increased by the irradiation, due to oxidation of DTT that was added to the protein solution to trap the generated nitrosobenzyl compound. Similar absorption changes were observed by irradiation of 355 nm laser pulses on a model molecule: *N*-acetyl-Asp-Gly-Cys modified with DMNB.

The structure of the DMNB-modified apoPC was examined by CD and 2D NMR measurements (Figures 2B and 3). By comparing the CD spectrum in the ultraviolet region of the DMNB-modified apoPC with that of the native apoPC,[46,47] it was found that the DMNB-modified apoPC possessed a denatured structure. The completely unfolded DMNB-modified apoPC at pH 2 showed a similar CD spectrum as that of acid or thermal denatured apoPC. To obtain more information on the three-dimensional structure of the DMNB-modified apoPC, we performed 2D NMR experiments on the modified protein. The 2D NMR spectrum of the DMNB-modified apoPC (Figure 3A) was similar to that reported for the unfolded apoPC,[33] with only weak signals representing a small fraction of folded protein, indicating that the modified apoPC is unfolded.

We irradiated UV light on the modified apoPC and measured the CD and NMR spectra at least 30 min after the irradiation (Figures 2B and 3B). The observed CD and NMR spectra converted back to those of the native β-sheet structure of apoPC. These results show that apoPC with a DMNB derivative of Cys exhibits a denatured structure and starts to refold with reconversion of the modified Cys to unlabeled Cys by irradiation of UV light according to the following reaction, which produces native apoPC and 4,5-dimethoxy-2-nitrosobenzaldehyde (DN):

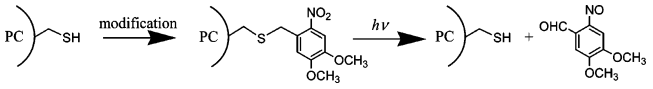

Since the DMNB group has an absorption band at 355 nm, which is isolated from the absorption band of the protein, it is possible to photocleave the DMNB group without exciting the protein part.

Rate of Photocleavage Reaction. The rate of the photocleavage reaction was monitored by the rise of the TG signal. Figure 4 shows the TG signals on microsecond time scale after photoexcitation of the DMNB-modified apoPC in 10 mM Na phosphate buffer, pH 7.4. The signal rises with a rate determined by the time response of our system (~20 ns), and then starts to rise more slowly. In the microsecond time range, the signal decays with a rate constant of $D_{th}q^2$. This decay component is identified with the thermal grating signal, which is produced by the thermal energy coming from the nonradiative transition and the enthalpy change of the reaction. The slow rise of the thermal grating signal can be fitted well by a single exponential function with a rate constant of 2.5×10^6 s^{-1}, which is

(46) Gross, E. L.; Draheim, J. E.; Curtiss, A. S.; Crombie, B.; Scheffer, A.; Pan, B.; Chiang, C.; Lopez, A. *Arch. Biochem. Biophys.* **1992**, *298*, 413−419.
(47) Bai, Y.; Chung, J.; Dyson, H. J.; Wright, P. E. *Protein Sci.* **2001**, *10*, 1056−1066.

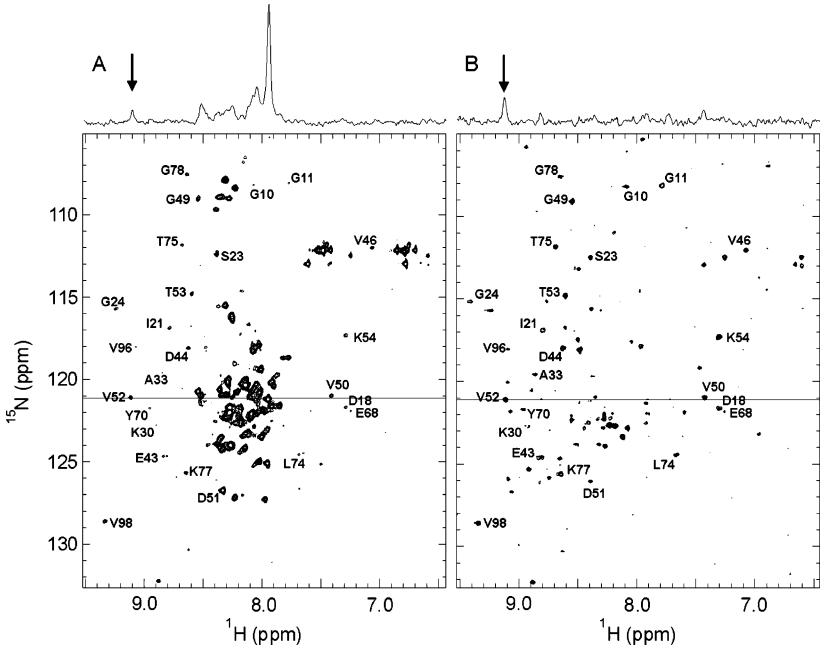

Figure 3. ^{15}N HSQC NMR spectra for the DMNB-modified apoPC (A) before and (B) after irradiation of 355 nm laser pulses. Assignments of some of the signals of the folded protein are indicated. ^{1}H traces were taken at the position of the horizontal lines, showing the resonance of Val52 (arrow). Note the strong signals of unfolded apoPC in panel A.

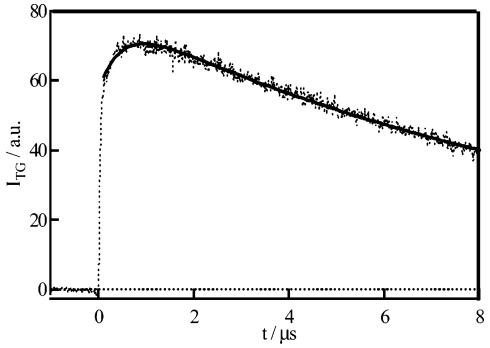

Figure 4. Transient grating signals (dotted line) after photoexcitation of the DMNB-modified apoPC in 10 mM Na phosphate buffer, pH 7.4, observed in microsecond time scale. The best fitted curve with a single exponential function for the slow rise component is shown by a solid line.

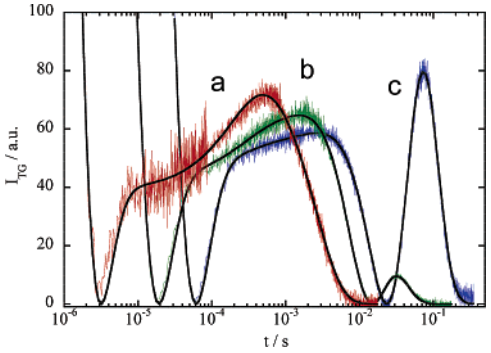

Figure 5. Transient grating signals after photoexcitation of the DMNB-modified apoPC in 10 mM Na phosphate buffer, pH 7.4, observed in wide time range at (a) $q^2 = 4.8 \times 10^{12}$ m^{-2} (red line), (b) $q^2 = 6.8 \times 10^{11}$ m^{-2} (green line), and (c) $q^2 = 2.1 \times 10^{11}$ m^{-2} (blue line). The best fitted curves with eq 3 for the signals are shown by the black lines. The initial fast decay component represents the decay of the thermal grating signal.

independent of q. This q-independent dynamics indicates that this component represents the reaction kinetics, and it is reasonable to attribute this component to the dissociation reaction of the substituent from apoPC. The time scale of this rise component indicates that the folding dynamics of DMNB-modified apoPC can be initiated on a time scale of 400 ns. We, therefore, can monitor the kinetics of the β-sheet formation in apoPC after 400 ns. However, we cannot observe the dynamics of the secondary structure formation if it is faster than 400 ns.

Volume Change. In a longer time region, the grating signal shows a rather complicated feature. Under a large q^2 condition (e.g., 4.8×10^{12} m^{-2}), the thermal grating signal decays to the baseline followed by other grow decay dynamics (Figure 5, curve a). The signal observed at this large q^2 can be expressed by a sum of four exponential functions:

$$I_{TG}(t) = \alpha[\delta n_{th}\exp(-D_{th}q^2t) + \delta n_1\exp(-k_1t) + \delta n_2\exp(-k_2t) + \delta n_3\exp(-k_3t)]^2 \quad (3)$$

where the first term represents the thermal grating term, δn_{th} is the refractive index change by the heating, $k_1 > k_2 > k_3$, $\delta n_{th} < 0$, $\delta n_1 < 0$, $\delta n_2 < 0$, and $\delta n_3 > 0$. All the terms except the thermal grating one represent the species gratings, which are due to the refractive index changes caused by creation or depletion of the chemical species by the photoexcitation. The assignment of the dynamics can be made by comparison of the TG signals under different q conditions. We found that k_1 does not depend on q ($k_1 = (3.7 \pm 0.3) \times 10^3$ s^{-1}), whereas k_2 and k_3 vary with q^2. The q-independent dynamics (k_1) should represent the nondiffusive dynamics of the species grating signal. There are mainly two dominant contributions in the species grating signal: population grating and volume grating. The population grating appears by the refractive index change accompanied with the absorption change, whereas the volume grating is created by the density change through the molecular volume change. Since the main absorption bands of apoPC are located in the UV region and the spectrum change after the photodissociation is negligible, the population grating contribution should be small. On the other hand, since the molecular

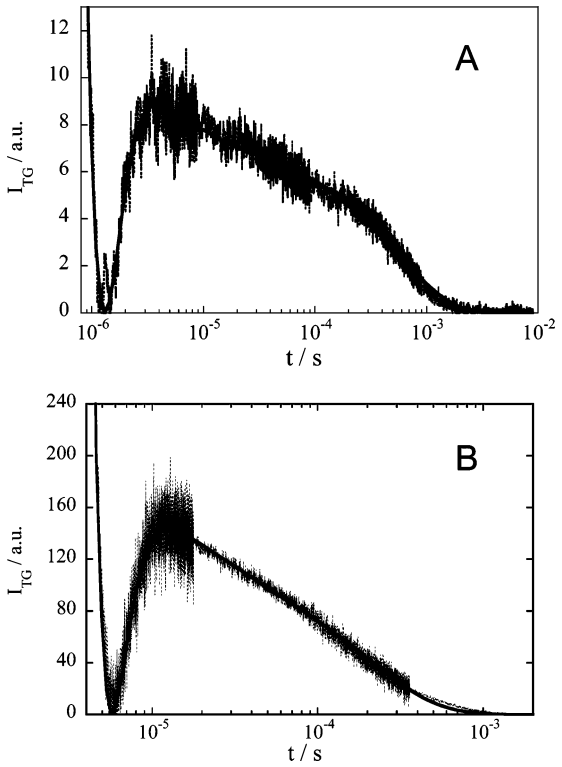

Figure 6. The TG signals (dotted lines) of (A) the DMNB-modified apoPC in the buffer with 0.8 M GdnHCl and (B) the modified model peptide (*N*-acetyl-Asp-Gly-Cys). The best fitted curves by (A) the triexponential and (B) biexponential functions with the thermal grating contribution are shown by the solid lines; q^2 values: *A*, 1.38×10^{13}; *B*, 4.32×10^{12}.

volume (partial molar volume) is expected to change during the folding of the protein, the observed grating signal is attributed to the volume change of apoPC. The negative sign of δn_1 indicates that the partial molar volume decreases by this process, that is, volume contraction.

There are several contributions in the partial molar volume change during the folding reaction, such as creation (or destruction) of voids and/or contact of atoms. The creation (destruction) of the void space should result in the volume increase (decrease), whereas contact of the atoms increases the free space of the solvent molecules and hence decreases the partial molecular volume. Because the void space should be minimum for the unfolded conformation, it is unlikely that the void space is destroyed during the protein folding. The observed volume contraction must represent the increase in the number of atomic contacts during the folding, which resulted from the collapse of the extended conformation of the unfolded apoPC. Therefore, the collapse of the structure occurs with a rate constant of 3.7×10^3 s^{-1}. It should be noted that this process represents a process from the initial state (U_1) to another unfolded intermediate state (U_2), which becomes apparent from the diffusion measurements as described below.

Substituent Dissociation from ApoPC. Since both modified and unlabeled apoPCs are denatured by an addition of 0.8 M GdnHCl as judged from the CD spectra (data not shown), the photoexcitation of the modified apoPC in the presence of 0.8 M GdnHCl should not induce the protein folding reaction. Indeed, a weak species grating signal was observed under this condition (Figure 6A), and the time profile of the species signal could be reproduced well by a sum of three exponential functions. From the rate constants, *D* of the three chemical species involved in this reaction were determined to be 1×10^{-8}, 6×10^{-10}, and 0.6×10^{-10} m^2 s^{-1}. As judged from the characteristic magnitudes of *D*, the species with the largest and smallest *D* values should be attributed to the proton and the denatured protein, respectively. Considering the photoproduct of the reaction, we should attribute the component with an intermediate *D* value to the diffusion of the final product, 4,5-dimethoxy-2-nitrosobenzaldehyde (DN). This assignment was further confirmed by the TG signal of the model molecule, *N*-acetyl-Asp-Gly-Cys modified with DMNB. The TG signal of this molecule shows the thermal grating and the species grating signals, of which the time profile can be reproduced well by a biexponential function (Figure 6B). From the rate constant, *D* of DN was determined to be 6×10^{-10} m^2 s^{-1}, which agrees quite well with the value determined for the modified apoPC in the presence of 0.8 M GdnHCl. Importantly, the species grating signals of DN from the modified apoPC as well as the model compound appear in a time range of 10−100 μs. The appearance of the free diffusion of DN strongly indicates that the photodissociation reaction is complete within 10 μs after the photoexcitation, and there is no interaction between DN and the protein after this time. Combining these results with the data of the 400 ns dynamics observed at the rise part of the thermal grating (Figure 3), we consider that DN is quickly released from the protein after the dissociation reaction. The TG signal due to DN, however, was undetectable during protein folding since the intensity of the DN signal was too weak compared with the signals from the protein.

Discussion

Change in Diffusion Coefficient of ApoPC during Folding. The *q*-dependent k_2 and k_3 dynamics in curve a of Figure 5 are attributed to the diffusion process. If *D* is constant during the observation time range, the rate constants of k_2 and k_3 should be given by Dq^2. The positive sign of δn_3 indicates that the chemical species, which diffuses with the rate constant of k_3, is a photocreated species (product in this time scale). Similarly, the species of the δn_2 component should be attributed to the depleted molecule by the photoexcitation, that is, the reactant (unfolded apoPC). From the values of k_2, k_3, and q^2, the diffusion coefficients of the initial unfolded apoPC (D_{U_1}) and the product (D_{U_2}) in the presented time range were determined to be $D_{U_1} = (0.81 \pm 0.05) \times 10^{-10}$ and $D_{U_2} = (0.45 \pm 0.05) \times 10^{-10}$ m^2 s^{-1}, respectively. Since these values are smaller than the *D* value of the benzyl group (ca. 6×10^{-10} m^2 s^{-1})[45] and even smaller than that of native apoPC ($D_N = 1.1 \times 10^{-10}$ m^2 s^{-1}; vide infra), both species should be attributed to unfolded apoPC. When apoPC is completely folded, *D* should be equal to D_N. Hence, the protein structure in the time range of 0−4 ms is not native but still unfolded in view of the *D* value.

We should note that D_{U_2} is smaller than D_{U_1} in this time range. Considering the rate of the volume contraction (3.7×10^3 s^{-1}), we found that *D* decreases even though the molecular size decreases. This observation seems to contradict the Stokes−Einstein formula, which predicts that *D* is inversely proportional to the molecular radius. However, as we will discuss later, *D* of apoPC is considered to be influenced by an intermolecular interaction, such as the hydrogen bonding. When the number of the hydrogen bonding increases, *D* should decrease. Therefore, D_{U_2} smaller than D_{U_1} indicates that the hydrogen bonding

network between the protein and water is enhanced temporarily at the earlier intermediate state U_2 during the protein folding process. If the volume contraction is induced by making the intramolecular hydrogen bond, we do not expect this slower diffusion for the intermediate. This result leads us to an idea that the volume contraction is caused by the hydrophobic collapse and not by the intramolecular hydrogen bonding formation. The reason the intermolecular hydrogen bonding is enhanced by the hydrophobic collapse is not clear at present. We may speculate that some hydrophobic side chains were exposed to the water before the collapse, and they might shield the hydrophilic side chains. By the hydrophobic collapse, the shielding effect of the water-exposed hydrophobic side chains would be reduced to increase the intermolecular interaction between the protein and the water molecules. Actually, the hydrophobic collapse has been reported in the folding processes of several proteins by experimental and simulation studies,[8,12,48−50] and the time scale observed for the collapse of apoPC is comparable with the time scales observed for other proteins.[8,48,50] Some local chain compaction of the unfolded apoPC has been observed as nanosecond time scale motional restriction for residues 17−24 and 57−64, which is presumably associated with transient formation of nonnative helical structures.[47]

Time Development of Intermolecular Interaction. It is particularly interesting to find that the signal feature is quite different in a smaller q region (Figure 5, curves b and c). After the thermal grating signal decays to the baseline, the TG signal shows two more rise-and-decay curves. If D is constant during the observation time range, the time profile of the TG signal should not depend on q. The different feature of the signal for different q (Figure 5, curves a−c) is a good indication that D is time-dependent in this observation time range (100 μs to 100 ms).[36,37] It is reasonable to consider that the time development of D is caused by the conformational change of the protein during the folding process.

We have analyzed the observed TG signal based on the following model. We assumed that the kinetics from U_2 to the third intermediate (U_3), which possesses a diffusion coefficient (D_{U_3}), is expressed by a single exponential function with a rate constant of k_D. This U_3 intermediate will be further folded to the native conformation with a rate constant corresponding to the slow isomerization reaction of the proline from the *trans* to the *cis* form.[32,33] Actually, the CD spectra continued to change for about 30 min after the UV irradiation on the modified apoPC (data not shown). This slow dynamics cannot be observed by the present TG method because the TG signal decays completely by the molecular diffusion process within a few hundred milliseconds. By solving the diffusion equations, we found that the changes in the refractive indexes for the U_2 (δn_{U_2}) and U_3 (δn_{U_3}) states can be expressed as[37,51]

$$\delta n_{U_2}(t) = \delta n^{o}_{U_2} \exp\{-(D_{U_2} q^2 + k_D)t\} \quad (4)$$

$$\delta n_{U_3}(t) = \delta n^{o}_{U_3} \frac{k_D}{(D_{U_3} - D_{U_2})q^2 - k_D} [\exp\{-(D_{U_2} q^2 + k_D)t\} - \exp(-D_{U_3} q^2 t)] \quad (5)$$

and the observed TG signal should be fitted by

$$I_{TG}(t) = \alpha[\delta n_{th} \exp(-D_{th} q^2 t) + \delta n_1 \exp(-k_1 t) + \delta n_{U_2}(t) + \delta n_{U_3}(t)]^2 \quad (6)$$

By fitting the signals obtained for various q, we found that D changes from $D_{U_2} = 0.45 \times 10^{-10}$ m^2 s^{-1} to $D_{U_3} = 1.1 \times 10^{-10}$ m^2 s^{-1} with a rate constant of $k_D = 43 \pm 3$ s^{-1}. In other words, the hydrodynamic radius is reduced by a factor of $D_{U_2}/D_{U_3} = 0.41$ with this rate. The reduction of the hydrodynamic radius is consistent with the protein packing from an extended unfolded intermediate (U_2) to a more compact intermediate (U_3), which could convert to native apoPC. However, this reduction of hydrodynamic radius may not be directly related to the geometrical change as described below.

The determined rate constant for the change of D during the folding process ($k_D = 43$ s^{-1}) is much smaller than that of the volume contraction ($k_1 = 3.7 \times 10^3$ s^{-1}). If D is determined by the molecular size as predicted by the Stokes−Einstein formula, both rates should coincide. The different rate leads us to consider that the hydrodynamic radius is not determined only by the protein conformation. Contrary to the radius of gyration, which is defined solely from the geometric structure, many factors contribute to the hydrodynamic radius. In this case, D reflects not only the size of the protein but also the intermolecular interaction. For example, even when the molecular size is the same, D (or the hydrodynamic radius) could be different depending on the intermolecular interaction between the solute and the solvent. The surface roughness may also affect the diffusion process. Since the hydrogen bonding interaction is a major intermolecular interaction in proteins, the hydrodynamic radius in this study should be considered as an indicator of the hydrogen bonding interaction and the shape of the protein, and not just the size of it. The enhancement of D from D_{U_2} to D_{U_3} indicates that the hydrogen bonding between the protein and water is changed from intermolecular to intramolecular hydrogen bonding with the rate constant of k_D. The study of the time-dependent D provides a unique opportunity to investigate the time development of the destruction (or formation) of hydrophobic or hydrogen bonding interaction during the folding dynamics.

Summary

The refolding process of apoPC is schematically summarized in Figure 7. After 400 ns of the laser irradiation, the protein is free to refold from the unfolded conformation. With a lifetime of 270 μs, the protein part collapses by the hydrophobic interaction. The intramolecular hydrogen bonding network is reformed with a rate constant of 43 s^{-1} leading to another intermediate species. This intermediate slowly converts to the native species by *trans*-to-*cis* isomerization of the two prolines, Pro16 and Pro36.[32] The present approach, time-dependent

(48) Chattopadhyay, K.; Zhong, S.; Yeh, S.-R.; Rousseau, D. L.; Frieden, C. *Biochemistry* **2002**, *41*, 4040−4047.
(49) Pollack, L.; Tate, M. W.; Darnton, N. C.; Knight, J. B.; Gruner, S. M.; Eaton, W. A.; Austin, R. H. *Proc. Natl. Acad. Sci. U.S.A.* **1999**, *96*, 10115−10117.
(50) Kuwata, K.; Shastry, R.; Cheng, H.; Hoshino, M.; Batt, C. A.; Goto, Y.; Roder, H. *Nat. Struct. Biol.* **2001**, *8*, 151−155.
(51) Choi, J.; Terazima, M. *Photochem. Photobiol. Sci.* **2003**, 767−773.

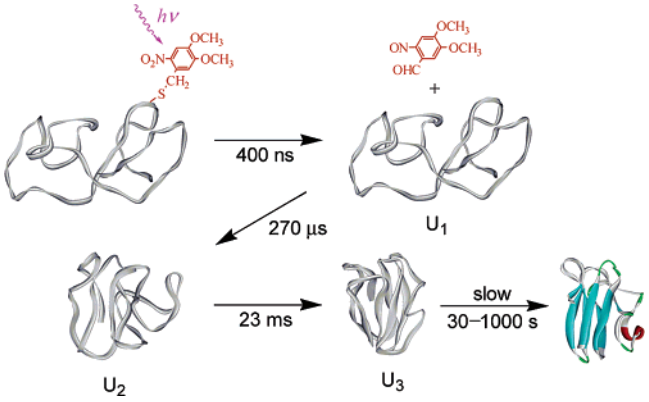

Figure 7. Schematic view of the apoPC refolding process initiated by removal of the DMNB group from modified apoPC by UV light irradiation. The red and blue colors represent the α-helical and *β*-sheet structures, respectively.

measurement of *D* with a light triggering method of protein folding, should be a unique and powerful way to study the protein folding kinetics from a viewpoint of the protein shape and the protein−water intermolecular interaction.

Acknowledgment. We thank Ms. Mika Minami and Ms. Kayo Azuma, Kyoto Pharmaceutical University, for help in the preparation and CD measurements of DMNB-modified apoPC. This work was supported by the Kurata Memorial Foundation, the Sumitomo Foundation, the Kowa Life Science Foundation, the Takeda Science Foundation, the Mitsubishi Chemical Corporation Fund, the Japan Science and Technology Agency (JST), and Grants-in-Aid (Nos. 164041242 and 16550149) to S.H. and (Nos. 13853002 and 15076204) to M.T. from the Ministry of Education, Culture, Sports, Science and Technology of Japan.

JA058788E